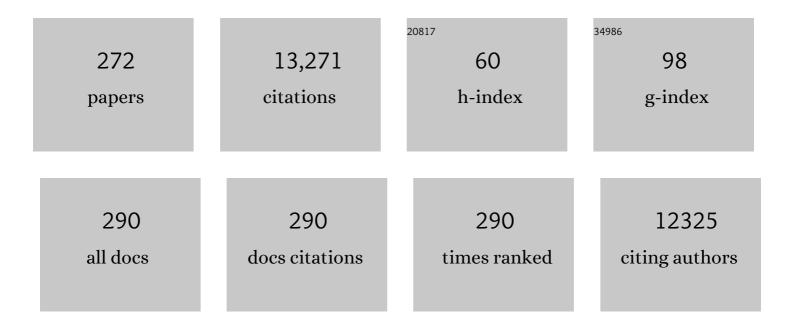
An-Min Zheng

List of Publications by Year in descending order

Source: https://exaly.com/author-pdf/1012575/publications.pdf Version: 2024-02-01



#	Article	IF	CITATIONS
1	BrÃ,nsted/Lewis Acid Synergy in Dealuminated HY Zeolite:  A Combined Solid-State NMR and Theoretical Calculation Study. Journal of the American Chemical Society, 2007, 129, 11161-11171.	13.7	349
2	Dependence of electronic structure of g-C 3 N 4 on the layer number of its nanosheets: A study by Raman spectroscopy coupled with first-principles calculations. Carbon, 2014, 80, 213-221.	10.3	331
3	Highly Mesoporous Single-Crystalline Zeolite Beta Synthesized Using a Nonsurfactant Cationic Polymer as a Dual-Function Template. Journal of the American Chemical Society, 2014, 136, 2503-2510.	13.7	266
4	Effects of Cellulose, Hemicellulose, and Lignin on the Structure and Morphology of Porous Carbons. ACS Sustainable Chemistry and Engineering, 2016, 4, 3750-3756.	6.7	261
5	³¹ P NMR Chemical Shifts of Phosphorus Probes as Reliable and Practical Acidity Scales for Solid and Liquid Catalysts. Chemical Reviews, 2017, 117, 12475-12531.	47.7	258
6	Understanding the High Photocatalytic Activity of (B, Ag)-Codoped TiO ₂ under Solar-Light Irradiation with XPS, Solid-State NMR, and DFT Calculations. Journal of the American Chemical Society, 2013, 135, 1607-1616.	13.7	230
7	2D and 3D Porphyrinic Covalent Organic Frameworks: The Influence of Dimensionality on Functionality. Angewandte Chemie - International Edition, 2020, 59, 3624-3629.	13.8	227
8	Acid properties of solid acid catalysts characterized by solid-state 31P NMR of adsorbed phosphorous probe molecules. Physical Chemistry Chemical Physics, 2011, 13, 14889.	2.8	204
9	Hydrophobic Solid Acids and Their Catalytic Applications in Green and Sustainable Chemistry. ACS Catalysis, 2018, 8, 372-391.	11.2	200
10	Direct Observation of Cyclic Carbenium Ions and Their Role in the Catalytic Cycle of the Methanolâ€toâ€Olefin Reaction over Chabazite Zeolites. Angewandte Chemie - International Edition, 2013, 52, 11564-11568.	13.8	193
11	Acidic Properties and Structure–Activity Correlations of Solid Acid Catalysts Revealed by Solid-State NMR Spectroscopy. Accounts of Chemical Research, 2016, 49, 655-663.	15.6	177
12	Insights into the Dealumination of Zeoliteâ€HY Revealed by Sensitivityâ€Enhanced ²⁷ Al DQâ€MAS NMR Spectroscopy at High Field. Angewandte Chemie - International Edition, 2010, 49, 8657-8661.	13.8	173
13	Catalytic dehydration of ethanol over post-treated ZSM-5 zeolites. Journal of Catalysis, 2014, 312, 204-215.	6.2	171
14	Boron Environments in B-Doped and (B, N)-Codoped TiO ₂ Photocatalysts: A Combined Solid-State NMR and Theoretical Calculation Study. Journal of Physical Chemistry C, 2011, 115, 2709-2719.	3.1	164
15	Comprehensive investigation of CO2 adsorption on Mg–Al–CO3 LDH-derived mixed metal oxides. Journal of Materials Chemistry A, 2013, 1, 12782.	10.3	164
16	Room temperature activation of methane over Zn modified H-ZSM-5 zeolites: Insight from solid-state NMR and theoretical calculations. Chemical Science, 2012, 3, 2932.	7.4	157
17	Isolated boron in zeolite for oxidative dehydrogenation of propane. Science, 2021, 372, 76-80.	12.6	155
18	BrÃ,nsted/Lewis Acid Synergy in H–ZSM-5 and H–MOR Zeolites Studied by ¹ H and ²⁷ Al DQ-MAS Solid-State NMR Spectroscopy. Journal of Physical Chemistry C, 2011, 115, 22320-22327.	3.1	147

#	Article	IF	CITATIONS
19	Mesoporous ZSM-5 Zeolite-Supported Ru Nanoparticles as Highly Efficient Catalysts for Upgrading Phenolic Biomolecules. ACS Catalysis, 2015, 5, 2727-2734.	11.2	147
20	Importance of Zeolite Wettability for Selective Hydrogenation of Furfural over Pd@Zeolite Catalysts. ACS Catalysis, 2018, 8, 474-481.	11.2	146
21	Significant Enhancement of C ₂ H ₂ /C ₂ H ₄ Separation by a Photochromic Diarylethene Unit: A Temperature―and Lightâ€Responsive Separation Switch. Angewandte Chemie - International Edition, 2017, 56, 7900-7906.	13.8	145
22	Theoretical Predictions of ³¹ P NMR Chemical Shift Threshold of Trimethylphosphine Oxide Absorbed on Solid Acid Catalysts. Journal of Physical Chemistry B, 2008, 112, 4496-4505.	2.6	143
23	Thermodynamic and molecular insights into the absorption of H ₂ S, CO ₂ , and CH ₄ in choline chloride plus urea mixtures. AICHE Journal, 2019, 65, e16574.	3.6	139
24	Insights into the Dual Activation Mechanism Involving Bifunctional Cinchona Alkaloid Thiourea Organocatalysts: An NMR and DFT Study. Journal of Organic Chemistry, 2012, 77, 9813-9825.	3.2	136
25	New Insight into the Hydrocarbonâ€Pool Chemistry of the Methanolâ€toâ€Olefins Conversion over Zeolite Hâ€ZSMâ€5 from GCâ€MS, Solidâ€State NMR Spectroscopy, and DFT Calculations. Chemistry - A European Journal, 2014, 20, 12432-12443.	3.3	131
26	Location, Acid Strength, and Mobility of the Acidic Protons in Keggin 12-H3PW12O40:  A Combined Solid-State NMR Spectroscopy and DFT Quantum Chemical Calculation Study. Journal of the American Chemical Society, 2005, 127, 18274-18280.	13.7	130
27	Thin-film composite membrane breaking the trade-off between conductivity and selectivity for a flow battery. Nature Communications, 2020, 11, 13.	12.8	127
28	Au-NHC@Porous Organic Polymers: Synthetic Control and Its Catalytic Application in Alkyne Hydration Reactions. ACS Catalysis, 2014, 4, 321-327.	11.2	124
29	Selective Catalytic Production of 5â€Hydroxymethylfurfural from Glucose by Adjusting Catalyst Wettability. ChemSusChem, 2014, 7, 402-406.	6.8	119
30	Origin and Structural Characteristics of Tri-coordinated Extra-framework Aluminum Species in Dealuminated Zeolites. Journal of the American Chemical Society, 2018, 140, 10764-10774.	13.7	113
31	Direct Insight into Ethane Oxidative Dehydrogenation over Boron Nitrides. ChemCatChem, 2017, 9, 3293-3297.	3.7	112
32	Probing the Spatial Proximities among Acid Sites in Dealuminated H-Y Zeolite by Solid-State NMR Spectroscopy. Journal of Physical Chemistry C, 2008, 112, 14486-14494.	3.1	105
33	Formation Pathway for LTA Zeolite Crystals Synthesized via a Charge Density Mismatch Approach. Journal of the American Chemical Society, 2013, 135, 2248-2255.	13.7	105
34	Acidic Strengths of BrÃ,nsted and Lewis Acid Sites in Solid Acids Scaled by ³¹ P NMR Chemical Shifts of Adsorbed Trimethylphosphine. Journal of Physical Chemistry C, 2011, 115, 7660-7667.	3.1	104
35	Mechanism of Myo-inositol Hexakisphosphate Sorption on Amorphous Aluminum Hydroxide: Spectroscopic Evidence for Rapid Surface Precipitation. Environmental Science & Technology, 2014, 48, 6735-6742.	10.0	103
36	Functional groups to modify g-C3N4 for improved photocatalytic activity of hydrogen evolution from water splitting. Chinese Chemical Letters, 2020, 31, 1648-1653.	9.0	99

#	Article	IF	CITATIONS
37	Influence of Acid Strength and Confinement Effect on the Ethylene Dimerization Reaction over Solid Acid Catalysts: A Theoretical Calculation Study. Journal of Physical Chemistry C, 2012, 116, 12687-12695.	3.1	96
38	Layered double hydroxide membrane with high hydroxide conductivity and ion selectivity for energy storage device. Nature Communications, 2021, 12, 3409.	12.8	94
39	³¹ P Chemical Shift of Adsorbed Trialkylphosphine Oxides for Acidity Characterization of Solid Acids Catalysts. Journal of Physical Chemistry A, 2008, 112, 7349-7356.	2.5	92
40	Extra-framework aluminium species in hydrated faujasite zeolite as investigated by two-dimensional solid-state NMR spectroscopy and theoretical calculations. Physical Chemistry Chemical Physics, 2010, 12, 3895.	2.8	92
41	Micro/nano-structured graphitic carbon nitride–Ag nanoparticle hybrids as surface-enhanced Raman scattering substrates with much improved long-term stability. Carbon, 2015, 87, 193-205.	10.3	86
42	Nitrogen-Decorated, Ordered Mesoporous Carbon Spheres as High-Efficient Catalysts for Selective Capture and Oxidation of H ₂ S. ACS Sustainable Chemistry and Engineering, 2019, 7, 7609-7618.	6.7	84
43	Theoretical Investigation of the Effects of the Zeolite Framework on the Stability of Carbenium Ions. Journal of Physical Chemistry C, 2011, 115, 7429-7439.	3.1	83
44	Thiol–chromene click chemistry: A coumarin-based derivative and its use as regenerable thiol probe and in bioimaging applications. Biosensors and Bioelectronics, 2013, 47, 300-306.	10.1	83
45	Relationship Between 1H Chemical Shifts of Deuterated Pyridinium Ions and BrÃ,nsted Acid Strength of Solid Acids. Journal of Physical Chemistry B, 2007, 111, 3085-3089.	2.6	82
46	Combined DFT Theoretical Calculation and Solid-State NMR Studies of Al Substitution and Acid Sites in Zeolite MCM-22. Journal of Physical Chemistry B, 2005, 109, 24273-24279.	2.6	80
47	Photoswitching adsorption selectivity in a diarylethene–azobenzene MOF. Chemical Communications, 2017, 53, 763-766.	4.1	80
48	One-pot template-free synthesis, growth mechanism and enhanced photocatalytic activity of monodisperse (BiO)2CO3 hierarchical hollow microspheres self-assembled with single-crystalline nanosheets. CrystEngComm, 2012, 14, 3534.	2.6	79
49	Design and synthesis of hydrophobic and stable mesoporous polymeric solid acid with ultra strong acid strength and excellent catalytic activities for biomass transformation. Applied Catalysis B: Environmental, 2013, 136-137, 193-201.	20.2	79
50	Ultrafast post-synthetic modification of a pillared cobalt(<scp>ii</scp>)-based metal–organic framework <i>via</i> sulfurization of its pores for high-performance supercapacitors. Journal of Materials Chemistry A, 2019, 7, 11953-11966.	10.3	72
51	Insight into dynamic and steady-state active sites for nitrogen activation to ammonia by cobalt-based catalyst. Nature Communications, 2020, 11, 653.	12.8	72
52	Acidity of Mesoporous MoOx/ZrO2and WOx/ZrO2Materials:Â A Combined Solid-State NMR and Theoretical Calculation Study. Journal of Physical Chemistry B, 2006, 110, 10662-10671.	2.6	70
53	Molecular elucidating of an unusual growth mechanism for polycyclic aromatic hydrocarbons in confined space. Nature Communications, 2020, 11, 1079.	12.8	70
54	Design and preparation of efficient hydroisomerization catalysts by the formation of stable SAPO-11 molecular sieve nanosheets with 10–20 nm thickness and partially blocked acidic sites. Chemical Communications, 2017, 53, 4942-4945.	4.1	69

#	Article	IF	CITATIONS
55	¹³ C Chemical Shift of Adsorbed Acetone for Measuring the Acid Strength of Solid Acids: A Theoretical Calculation Study. Journal of Physical Chemistry C, 2010, 114, 12711-12718.	3.1	67
56	Efficient biomass transformations catalyzed by graphene-like nanoporous carbons functionalized with strong acid ionic liquids and sulfonic groups. Green Chemistry, 2015, 17, 480-489.	9.0	64
57	A Heterogeneous Metalâ€Free Catalyst for Hydrogenation: Lewis Acid–Base Pairs Integrated into a Carbon Lattice. Angewandte Chemie - International Edition, 2018, 57, 13800-13804.	13.8	64
58	Identification of <i>tert</i> â€Butyl Cations in Zeolite Hâ€ZSMâ€5: Evidence from NMR Spectroscopy and DFT Calculations. Angewandte Chemie - International Edition, 2015, 54, 8783-8786.	13.8	63
59	Acidity characterization of heterogeneous catalysts by solid-state NMR spectroscopy using probe molecules. Solid State Nuclear Magnetic Resonance, 2013, 55-56, 12-27.	2.3	62
60	Experimental Evidence on the Formation of Ethene through Carbocations in Methanol Conversion over Hâ€ZSMâ€5 Zeolite. Chemistry - A European Journal, 2015, 21, 12061-12068.	3.3	62
61	In situ imaging of the sorption-induced subcell topological flexibility of a rigid zeolite framework. Science, 2022, 376, 491-496.	12.6	62
62	¹⁹ F Chemical Shift of Crystalline Metal Fluorides: Theoretical Predictions Based on Periodic Structure Models. Journal of Physical Chemistry C, 2009, 113, 15018-15023.	3.1	61
63	Design of Efficient, Hierarchical Porous Polymers Endowed with Tunable Structural Base Sites for Direct Catalytic Elimination of COS and H ₂ S. ACS Applied Materials & Interfaces, 2019, 11, 29950-29959.	8.0	61
64	Molecular Routes of Dynamic Autocatalysis for Methanol-to-Hydrocarbons Reaction. Journal of the American Chemical Society, 2021, 143, 12038-12052.	13.7	60
65	Synthesis and memory characteristics of polyimides containing noncoplanar aryl pendant groups. Polymer, 2012, 53, 229-240.	3.8	59
66	Zirconium Oxide Supported Palladium Nanoparticles as a Highly Efficient Catalyst in the Hydrogenation–Amination of Levulinic Acid to Pyrrolidones. ChemCatChem, 2017, 9, 2661-2667.	3.7	59
67	Methanol to Olefins Reaction over Cavity-type Zeolite: Cavity Controls the Critical Intermediates and Product Selectivity. ACS Catalysis, 2018, 8, 10950-10963.	11.2	59
68	Differentiating Surface Ce Species among CeO ₂ Facets by Solid-State NMR for Catalytic Correlation. ACS Catalysis, 2020, 10, 4003-4011.	11.2	59
69	Combined spectral experiment and theoretical calculation to study the chemosensors of copper and their applications in anion bioimaging. Sensors and Actuators B: Chemical, 2013, 177, 1189-1197.	7.8	58
70	Two-dimensional graphitic C ₃ N ₅ materials: promising metal-free catalysts and CO ₂ adsorbents. Journal of Materials Chemistry A, 2018, 6, 7168-7174.	10.3	58
71	Methanol to Olefins Reaction Route Based on Methylcyclopentadienes as Critical Intermediates. ACS Catalysis, 2019, 9, 7373-7379.	11.2	58
72	Combined Solid-State NMR and Theoretical Calculation Studies of BrÃ,nsted Acid Properties in Anhydrous 12-Molybdophosphoric Acid. Journal of Physical Chemistry C, 2010, 114, 15464-15472.	3.1	57

#	Article	IF	CITATIONS
73	Phosphotungstic acid loaded on hydrophilic ionic liquid modified SBA-15 for selective oxidation of alcohols with aqueous H2O2. Microporous and Mesoporous Materials, 2012, 158, 77-87.	4.4	57
74	Methanol to hydrocarbons reaction over Hβ zeolites studied by high resolution solid-state NMR spectroscopy: Carbenium ions formation and reaction mechanism. Journal of Catalysis, 2016, 335, 47-57.	6.2	57
75	Spies Within Metal-Organic Frameworks: Investigating Metal Centers Using Solid-State NMR. Journal of Physical Chemistry C, 2014, 118, 23728-23744.	3.1	56
76	BrÃ,nsted/Lewis acid sites synergistically promote the initial C–C bond formation in the MTO reaction. Chemical Science, 2018, 9, 6470-6479.	7.4	56
77	Post-synthesis, characterization and catalytic properties of fluorine-planted MWW-type titanosilicate. Physical Chemistry Chemical Physics, 2013, 15, 4930.	2.8	55
78	Nonvolatile memory devices based on polyimides bearing noncoplanar twisted biphenyl units containing carbazole and triphenylamine side-chain groups. Journal of Materials Chemistry, 2011, 21, 15643.	6.7	54
79	An Extraâ€Largeâ€Pore Zeolite with 24×8×8â€Ring Channels Using a Structureâ€Directing Agent Derived fror Traditional Chinese Medicine. Angewandte Chemie - International Edition, 2018, 57, 6486-6490.	n 13.8	54
80	Roles of 8-ring and 12-ring channels in mordenite for carbonylation reaction: From the perspective of molecular adsorption and diffusion. Journal of Catalysis, 2019, 369, 335-344.	6.2	54
81	Solid-state 31P NMR mapping of active centers and relevant spatial correlations in solid acid catalysts. Nature Protocols, 2020, 15, 3527-3555.	12.0	54
82	Depolymerization of crystalline cellulose catalyzed by acidic ionic liquids grafted onto sponge-like nanoporous polymers. Chemical Communications, 2013, 49, 8456.	4.1	53
83	Unravelling the Efficient Photocatalytic Activity of Boron-induced Ti3+ Species in the Surface Layer of TiO2. Scientific Reports, 2016, 6, 34765.	3.3	53
84	Origin of weak Lewis acids on silanol nests in dealuminated zeolite Beta. Journal of Catalysis, 2019, 380, 204-214.	6.2	53
85	Graphene activated 3D-hierarchical flower-like Li ₂ FeSiO ₄ for high-performance lithium-ion batteries. Journal of Materials Chemistry A, 2015, 3, 16567-16573.	10.3	52
86	Transformation synthesis of aluminosilicate SSZ-39 zeolite from ZSM-5 and beta zeolite. Journal of Materials Chemistry A, 2019, 7, 4420-4425.	10.3	52
87	Slight channel difference influences the reaction pathway of methanol-to-olefins conversion over acidic H-ZSM-22 and H-ZSM-12 zeolites. Catalysis Science and Technology, 2015, 5, 3507-3517.	4.1	51
88	Interconnected hierarchical HUSY zeolite-loaded Ni nano-particles probed for hydrodeoxygenation of fatty acids, fatty esters, and palm oil. Journal of Materials Chemistry A, 2016, 4, 11330-11341.	10.3	51
89	Fischer–Tropsch synthesis to olefins boosted by MFI zeolite nanosheets. Nature Nanotechnology, 2022, 17, 714-720.	31.5	51
90	Fluorine-planted titanosilicate with enhanced catalytic activity in alkene epoxidation with hydrogen peroxide. Catalysis Science and Technology, 2012, 2, 2433.	4.1	50

#	Article	IF	CITATIONS
91	Diffusion Dependence of the Dual-Cycle Mechanism for MTO Reaction Inside ZSM-12 and ZSM-22 Zeolites. Journal of Physical Chemistry C, 2017, 121, 22872-22882.	3.1	50
92	Reactivity Enhancement of 2-Propanol Photocatalysis on SO ₄ ^{2â^'} /TiO ₂ : Insights from Solid-State NMR Spectroscopy. Environmental Science & Technology, 2008, 42, 5316-5321.	10.0	49
93	Interaction between Histidine and Zn(II) Metal Ions over a Wide pH as Revealed by Solid-State NMR Spectroscopy and DFT Calculations. Journal of Physical Chemistry B, 2013, 117, 8954-8965.	2.6	48
94	Tuning the pore structure of plug-containing Al-SBA-15 by post-treatment and its selectivity for C16 olefin in ethylene oligomerization. Microporous and Mesoporous Materials, 2014, 184, 151-161.	4.4	47
95	A novel recognition mechanism supported by experiment and theoretical calculation for hypochlorites recognition and its practical application. Sensors and Actuators B: Chemical, 2016, 224, 307-314.	7.8	47
96	Porous organic materials with ultra-small pores and sulfonic functionality for xenon capture with exceptional selectivity. Journal of Materials Chemistry A, 2018, 6, 11163-11168.	10.3	47
97	Higher Magnetic Fields, Finer MOF Structural Information: ¹⁷ O Solid-State NMR at 35.2 T. Journal of the American Chemical Society, 2020, 142, 14877-14889.	13.7	47
98	Mapping Out Chemically Similar, Crystallographically Nonequivalent Hydrogen Sites in Metal‑Organic Frameworks by ¹ H Solid-State NMR Spectroscopy. Chemistry of Materials, 2015, 27, 3306-3316.	6.7	46
99	Removal and safe reuse of highly toxic allyl alcohol using a highly selective photo-sensitive metal–organic framework. Green Chemistry, 2016, 18, 2047-2055.	9.0	46
100	Cavity-controlled diffusion in 8-membered ring molecular sieve catalysts for shape selective strategy. Journal of Catalysis, 2019, 377, 51-62.	6.2	45
101	Molecular Understanding of the Catalytic Consequence of Ketene Intermediates under Confinement. Journal of the American Chemical Society, 2021, 143, 15440-15452.	13.7	45
102	Pore Selectivity for Olefin Protonation Reactions Confined inside Mordenite Zeolite: A Theoretical Calculation Study. Journal of Physical Chemistry C, 2013, 117, 2194-2202.	3.1	43
103	New Insights into Kegginâ€Type 12â€Tungstophosphoric Acid from ³¹ P MAS NMR Analysis of Absorbed Trimethylphosphine Oxide and DFT Calculations. Chemistry - an Asian Journal, 2011, 6, 137-148.	3.3	42
104	New Insights into the Effects of Acid Strength on the Solid Acid-Catalyzed Reaction: Theoretical Calculation Study of Olefinic Hydrocarbon Protonation Reaction. Journal of Physical Chemistry C, 2010, 114, 10254-10264.	3.1	41
105	Presituated "coke―determined mechanistic route for ethene formation in the methanol-to-olefins process on SAPO-34 catalyst. Journal of Catalysis, 2019, 377, 153-162.	6.2	40
106	Influence of acid strength on the reactivity of alkane activation on solid acid catalysts: A theoretical calculation study. Microporous and Mesoporous Materials, 2012, 151, 241-249.	4.4	39
107	Potassium-directed sustainable synthesis of new high silica small-pore zeolite with KFI structure (ZJM-7) as an efficient catalyst for NH3-SCR reaction. Applied Catalysis B: Environmental, 2021, 281, 119480.	20.2	39
108	Chemoselectivity during propene hydrogenation reaction over H-ZSM-5 zeolite: Insights from theoretical calculations. Microporous and Mesoporous Materials, 2009, 121, 158-165.	4.4	38

#	Article	IF	CITATIONS
109	Polyoxometalate-based ionic complexes immobilized in mesoporous silicas prepared via a one-pot procedure: Efficient and reusable catalysts for H2O2-mediated alcohol oxidations in aqueous media. Microporous and Mesoporous Materials, 2013, 172, 67-76.	4.4	38
110	Highly nitrogen-doped mesoscopic carbons as efficient metal-free electrocatalysts for oxygen reduction reactions. Journal of Materials Chemistry A, 2014, 2, 20030-20037.	10.3	37
111	Developing two-dimensional solid superacids with enhanced mass transport, extremely high acid strength and superior catalytic performance. Chemical Science, 2019, 10, 5875-5883.	7.4	37
112	Identification of Three Novel Polyphenolic Compounds, Origanine A–C, with Unique Skeleton from <i>Origanum vulgare</i> L. Using the Hyphenated LC-DAD-SPE-NMR/MS Methods. Journal of Agricultural and Food Chemistry, 2012, 60, 129-135.	5.2	36
113	A single Au nanoparticle anchored inside the porous shell of periodic mesoporous organosilica hollow spheres. Nano Research, 2015, 8, 3404-3411.	10.4	36
114	Fish-in-hole: rationally positioning palladium into traps of zeolite crystals for sinter-resistant catalysts. Chemical Communications, 2018, 54, 3274-3277.	4.1	36
115	Carbocation chemistry confined in zeolites: spectroscopic and theoretical characterizations. Chemical Society Reviews, 2022, 51, 4337-4385.	38.1	36
116	Enhancement of BrÃ,nsted acidity in zeolitic catalysts due to an intermolecular solvent effect in confined micropores. Chemical Communications, 2012, 48, 6936.	4.1	35
117	Sizable dynamics in small pores: CO ₂ location and motion in the α-Mg formate metal–organic framework. Physical Chemistry Chemical Physics, 2017, 19, 6130-6141.	2.8	35
118	Mass Transfer Advantage of Hierarchical Zeolites Promotes Methanol Converting into <i>para</i> -Methyl Group in Toluene Methylation. Industrial & Engineering Chemistry Research, 2017, 56, 9310-9321.	3.7	35
119	Effective transformation of cellulose to 5-hydroxymethylfurfural catalyzed by fluorine anion-containing ionic liquid modified biochar sulfonic acids in water. Cellulose, 2017, 24, 95-106.	4.9	35
120	From One to Two: Acidic Proton Spatial Networks in Porous Zeolite Materials. Chemistry of Materials, 2020, 32, 1332-1342.	6.7	35
121	Promising long-lasting phosphor material: a novel metal–organic framework showing intriguing luminescent performance. Dalton Transactions, 2012, 41, 13280.	3.3	34
122	Photoswitching storage of guest molecules in metal–organic framework for photoswitchable catalysis: exceptional product, ultrahigh photocontrol, and photomodulated size selectivity. Journal of Materials Chemistry A, 2017, 5, 7961-7967.	10.3	34
123	Direct Synthesis of Aluminosilicate SSZ-39 Zeolite Using Colloidal Silica as a Starting Source. ACS Applied Materials & Interfaces, 2019, 11, 23112-23117.	8.0	34
124	Effect of coking and propylene adsorption on enhanced stability for Co2+-catalyzed propane dehydrogenation. Journal of Catalysis, 2021, 395, 105-116.	6.2	34
125	Progress in development and application of solid-state NMR for solid acid catalysis. Chinese Journal of Catalysis, 2013, 34, 436-491.	14.0	33
126	Size-dependent sorption of myo-inositol hexakisphosphate and orthophosphate on nano-γ-Al2O3. Journal of Colloid and Interface Science, 2015, 451, 85-92.	9.4	33

#	Article	IF	CITATIONS
127	Strong or weak acid, which is more efficient for Beckmann rearrangement reaction over solid acid catalysts?. Catalysis Science and Technology, 2015, 5, 3675-3681.	4.1	32
128	Template-free synthesis of porous carbonaceous solid acids with controllable acid sites and their excellent activity for catalyzing the synthesis of biofuels and fine chemicals. Catalysis Science and Technology, 2016, 6, 2995-3007.	4.1	32
129	Analyzing Gas Adsorption in an Amide-Functionalized Metal Organic Framework: Are the Carbonyl or Amine Groups Responsible?. Chemistry of Materials, 2018, 30, 3613-3617.	6.7	32
130	Accelerating Biodiesel Catalytic Production by Confined Activation of Methanol over High-Concentration Ionic Liquid-Grafted UiO-66 Solid Superacids. ACS Catalysis, 2020, 10, 11848-11856.	11.2	32
131	Simultaneous Evaluation of Reaction and Diffusion over Molecular Sieves for Shape-Selective Catalysis. ACS Catalysis, 2020, 10, 8727-8735.	11.2	32
132	Formation, Location, and Photocatalytic Reactivity of Methoxy Species on Keggin 12-H ₃ PW ₁₂ O ₄₀ : A Joint Solid-State NMR Spectroscopy and DFT Calculation Study. Journal of Physical Chemistry C, 2008, 112, 15765-15770.	3.1	31
133	Host–Guest Interactions in Dealuminated HY Zeolite Probed by ¹³ C– ²⁷ Al Solid-State NMR Spectroscopy. Journal of Physical Chemistry Letters, 2014, 5, 3068-3072.	4.6	31
134	Anionic Clusters Enhanced Catalytic Performance of Protic Acid Ionic Liquids for Isobutane Alkylation. Industrial & Engineering Chemistry Research, 2016, 55, 8271-8280.	3.7	31
135	Design and synthesis of micro–meso–macroporous polymers with versatile active sites and excellent activities in the production of biofuels and fine chemicals. Green Chemistry, 2016, 18, 6536-6544.	9.0	30
136	Influences of the confinement effect and acid strength of zeolite on the mechanisms of Methanol-to-Olefins conversion over H-ZSM-5: A theoretical study of alkenes-based cycle. Microporous and Mesoporous Materials, 2016, 231, 216-229.	4.4	30
137	Direct Synthesis of Aluminosilicate IWR Zeolite from a Strong Interaction between Zeolite Framework and Organic Template. Journal of the American Chemical Society, 2019, 141, 18318-18324.	13.7	30
138	Brönsted and Lewis Acidity of the BF3/γ-Al2O3Alkylation Catalyst as Revealed by Solid-State NMR Spectroscopy and DFT Quantum Chemical Calculations. Journal of Physical Chemistry B, 2005, 109, 13124-13131.	2.6	29
139	¹³ C shielding tensors of crystalline amino acids and peptides: Theoretical predictions based on periodic structure models. Journal of Computational Chemistry, 2009, 30, 222-235.	3.3	29
140	Insight into the formation of the tert-butyl cation confined inside H-ZSM-5 zeolite from NMR spectroscopy and DFT calculations. Chemical Communications, 2016, 52, 10606-10608.	4.1	29
141	Prediction of the 13C NMR chemical shifts of organic species adsorbed on H-ZSM-5 zeolite by the ONIOM-GIAO method. Chemical Communications, 2005, , 2474.	4.1	28
142	Significant photocatalytic activity enhancement of titania inverse opals by anionic impurities removal in dye molecule degradation. Applied Catalysis B: Environmental, 2013, 138-139, 219-228.	20.2	28
143	Direct observation of methylcyclopentenyl cations (MCP ⁺) and olefin generation in methanol conversion over TON zeolite. Catalysis Science and Technology, 2016, 6, 89-97.	4.1	28
144	13C NMR shielding tensors of carboxyl carbon in amino acids calculated by ONIOM method. Chemical Physics Letters, 2004, 399, 172-176.	2.6	27

#	Article	IF	CITATIONS
145	DFT studies on the reaction mechanism of cross-metathesis of ethylene and 2-butylene to propylene over heterogeneous Mo/HBeta catalyst. Journal of Molecular Catalysis A, 2010, 330, 99-106.	4.8	27
146	Ordered Mesoporous Polymers for Biomass Conversions and Crossâ€Coupling Reactions. ChemSusChem, 2016, 9, 2496-2504.	6.8	27
147	An NMR Scale for Measuring the Base Strength of Solid Catalysts with Pyrrole Probe: A Combined Solid-State NMR Experiment and Theoretical Calculation Study. Journal of Physical Chemistry C, 2017, 121, 3887-3895.	3.1	27
148	Ultrathin nanosheets of aluminosilicate FER zeolites synthesized in the presence of a sole small organic ammonium. Journal of Materials Chemistry A, 2019, 7, 16671-16676.	10.3	27
149	Mesoporous MSU materials functionalized with sulfonic group: A multinuclear NMR and theoretical calculation study. Microporous and Mesoporous Materials, 2006, 89, 219-226.	4.4	26
150	Highly efficient single-layer organic light-emitting devices using cationic iridium complex as host. Organic Electronics, 2013, 14, 744-753.	2.6	26
151	Methanol carbonylation over copper-modified mordenite zeolite: A solid-state NMR study. Solid State Nuclear Magnetic Resonance, 2016, 80, 1-6.	2.3	26
152	External or internal surface of H-ZSM-5 zeolite, which is more effective for the Beckmann rearrangement reaction?. Catalysis Science and Technology, 2017, 7, 2512-2523.	4.1	26
153	Pd@Zn-MOF-74: Restricting a Guest Molecule by the Open-Metal Site in a Metal–Organic Framework for Selective Semihydrogenation. Inorganic Chemistry, 2018, 57, 12444-12447.	4.0	26
154	Gating Mechanism of Aquaporin Z in Synthetic Bilayers and Native Membranes Revealed by Solid-State NMR Spectroscopy. Journal of the American Chemical Society, 2018, 140, 7885-7895.	13.7	26
155	A Molecular Ferroelectric Showing Roomâ€Temperature Recordâ€Fast Switching of Spontaneous Polarization. Angewandte Chemie - International Edition, 2018, 57, 9833-9837.	13.8	26
156	Waterâ€Induced Structural Dynamic Process in Molecular Sieves under Mild Hydrothermal Conditions: Shipâ€Inâ€Bâ€Bottle Strategy for Acidity Identification and Catalyst Modification. Angewandte Chemie - International Edition, 2020, 59, 20672-20681.	13.8	26
157	pH-sensitive fluorescent salicylaldehyde derivative for selective imaging of hydrogen sulfide in living cells. Sensors and Actuators B: Chemical, 2013, 186, 212-218.	7.8	25
158	Solid-state NMR Studies of Host–Guest Interaction between UiO-67 and Light Alkane at Room Temperature. Journal of Physical Chemistry C, 2017, 121, 14261-14268.	3.1	25
159	Highly Efficient Indirect Hydration of Olefins to Alcohols Using Superacidic Polyoxometalate-Based Ionic Hybrids Catalysts. Industrial & Engineering Chemistry Research, 2018, 57, 6654-6663.	3.7	25
160	Reaction Route and Mechanism of the Direct N-Alkylation of Sulfonamides on Acidic Mesoporous Zeolite β-Catalyst. ACS Catalysis, 2018, 8, 9043-9055.	11.2	25
161	High population and dispersion of pentacoordinated AIV species on the surface of flame-made amorphous silica-alumina. Science Bulletin, 2019, 64, 516-523.	9.0	25
162	Tristable data storage device of soluble polyimides based on novel asymmetrical diamines containing carbazole. Polymer Chemistry, 2016, 7, 1765-1772.	3.9	24

#	Article	IF	CITATIONS
163	Rationally designing mixed Cu–(μ-O)–M (M = Cu, Ag, Zn, Au) centers over zeolite materials with high catalytic activity towards methane activation. Physical Chemistry Chemical Physics, 2018, 20, 26522-26531.	2.8	24
164	A porous BrÃ,nsted superacid as an efficient and durable solid catalyst. Journal of Materials Chemistry A, 2018, 6, 18712-18719.	10.3	24
165	Thermal resistance effect on anomalous diffusion of molecules under confinement. Proceedings of the United States of America, 2021, 118, .	7.1	24
166	The first carbon-carbon bond formation mechanism in methanol-to-hydrocarbons process over chabazite zeolite. CheM, 2021, 7, 2415-2428.	11.7	24
167	Design of a Small Organic Template for the Synthesis of Self-Pillared Pentasil Zeolite Nanosheets. Journal of the American Chemical Society, 2022, 144, 6270-6277.	13.7	24
168	Stability of the Reaction Intermediates of Ethylbenzene Disproportionation over Medium-Pore Zeolites with Different Framework Topologies: A Theoretical Investigation. Journal of Physical Chemistry C, 2013, 117, 23626-23637.	3.1	23
169	Mercaptosilane-assisted synthesis of sub-nanosized Pt particles within hierarchically porous ZSM-5/SBA-15 materials and their enhanced hydrogenation properties. Nanoscale, 2015, 7, 10918-10924.	5.6	23
170	Violation or Abidance of Löwenstein's Rule in Zeolites Under Synthesis Conditions?. ACS Catalysis, 2019, 9, 10618-10625.	11.2	23
171	Acid–base synergistic catalysis of biochar sulfonic acid bearing polyamide for microwave-assisted hydrolysis of cellulose in water. Cellulose, 2019, 26, 751-762.	4.9	22
172	Dependence of zeolite topology on alkane diffusion inside <scp> diverse channels</scp> . AICHE Journal, 2020, 66, e16269.	3.6	22
173	A Cationic Oligomer as an Organic Template for Direct Synthesis of Aluminosilicate ITH Zeolite. Angewandte Chemie - International Edition, 2020, 59, 15649-15655.	13.8	22
174	Surface Fingerprinting of Faceted Metal Oxides and Porous Zeolite Catalysts by Probe-Assisted Solid-State NMR Approaches. Accounts of Chemical Research, 2021, 54, 2421-2433.	15.6	21
175	Enhanced hydrothermal stability of Cu/SSZ-39 with increasing Cu contents, and the mechanism of selective catalytic reduction of NO. Microporous and Mesoporous Materials, 2021, 320, 111060.	4.4	21
176	Efficiently Selective Oxidation of H ₂ S to Elemental Sulfur over Covalent Triazine Framework Catalysts. ACS Applied Materials & Interfaces, 2021, 13, 34124-34133.	8.0	21
177	Acidity Characterization of Solid Acid Catalysts by Solid-State 31P NMR of Adsorbed Phosphorus-Containing Probe Molecules. Annual Reports on NMR Spectroscopy, 2014, 81, 47-108.	1.5	20
178	Preparation of Mesoporous Zeolite ETSâ€10 Catalysts for High‥ield Synthesis of α,βâ€Epoxy Ketones. ChemCatChem, 2015, 7, 521-525.	3.7	20
179	Identifying the effective phosphorous species over modified P-ZSM-5 zeolite: a theoretical study. Physical Chemistry Chemical Physics, 2018, 20, 11702-11712.	2.8	20
180	Reactivity descriptors of diverse copper-oxo species on ZSM-5 zeolite towards methane activation. Catalysis Today, 2019, 338, 108-116.	4.4	20

#	Article	IF	CITATIONS
181	Anionic Tuning of Zeolite Crystallization. CCS Chemistry, 2021, 3, 189-198.	7.8	20
182	Induced Active Sites by Adsorbate in Zeotype Materials. Journal of the American Chemical Society, 2021, 143, 8761-8771.	13.7	19
183	Mechanism of alkane H/D exchange over zeolite H-ZSM-5 at low temperature: a combined computational and experimental study. Catalysis Science and Technology, 2016, 6, 5350-5363.	4.1	18
184	High Activity of Amine-Doped H-ZSM-5 Zeolite in Ethene Protonation: Revealed by Embedding Calculations. ChemPhysChem, 2007, 8, 231-234.	2.1	17
185	Insight into the effects of acid characteristics on the catalytic performance of Sn-MFI zeolites in the transformation of dihydroxyacetone to methyl lactate. Journal of Catalysis, 2020, 391, 386-396.	6.2	17
186	Synergistically enhance confined diffusion by continuum intersecting channels in zeolites. Science Advances, 2021, 7, .	10.3	17
187	The Effect of Support Acidity on Olefin Metathesis over Heterogeneous Mo/HBeta Catalyst: A DFT Study. Catalysis Letters, 2010, 138, 116-123.	2.6	16
188	Plug precursor assisted synthesis: A highly efficient method of tuning the acidic and structural properties of Al-SBA-15. Microporous and Mesoporous Materials, 2015, 207, 111-119.	4.4	16
189	In Situ Observation of Nonâ€Classical 2â€Norbornyl Cation in Confined Zeolites at Ambient Temperature. Angewandte Chemie - International Edition, 2021, 60, 4581-4587.	13.8	16
190	A Cationic Polymerization Strategy to Design Sulfonated Micro–Mesoporous Polymers as Efficient Adsorbents for Ammonia Capture and Separation. Macromolecules, 2021, 54, 7010-7020.	4.8	16
191	DFT Study on the NMR Chemical Shifts of Molecules Confined in Carbon Nanotubes. Journal of Physical Chemistry C, 2013, 117, 23418-23424.	3.1	15
192	Exploring the ring current of carbon nanotubes by first-principles calculations. Chemical Science, 2015, 6, 902-908.	7.4	15
193	Lithium doping on 2D squaraine-bridged covalent organic polymers for enhancing adsorption properties: a theoretical study. Physical Chemistry Chemical Physics, 2018, 20, 6487-6499.	2.8	15
194	<i>N-</i> Oxyl Radicals Trapped on Zeolite Surface Accelerate Photocatalysis. ACS Catalysis, 2019, 9, 10448-10453.	11.2	15
195	Cooperative catalytically active sites for methanol activation by single metal ion-doped H-ZSM-5. Chemical Science, 2021, 12, 210-219.	7.4	15
196	Acidic hierarchical porous ZSM-5 assembled palladium catalyst: A green substitute to transform primary amides to nitriles. Applied Catalysis B: Environmental, 2022, 302, 120835.	20.2	15
197	Regioselectivity of carbonium ion transition states in zeolites. Catalysis Today, 2011, 164, 40-45.	4.4	14
198	Optimization of Reaction Conditions towards Multiple Types of Framework Isomers and Periodicâ€Increased Porosity: Luminescence Properties and Selective CO ₂ Adsorption over N ₂ . ChemPhysChem, 2013, 14, 3594-3599.	2.1	14

#	Article	IF	CITATIONS
199	Investigation of the Strong BrÃ,nsted Acidity in a Novel SAPO-type Molecular Sieve, DNL-6. Journal of Physical Chemistry C, 2015, 119, 2589-2596.	3.1	14
200	Direct synthesis of the organic and Ge free Al containing BOG zeolite (ITQ-47) and its application for transformation of biomass derived molecules. Chemical Science, 2020, 11, 12103-12108.	7.4	14
201	Dynamic Activation of C1 Molecules Evoked by Zeolite Catalysis. ACS Central Science, 2021, 7, 681-687.	11.3	14
202	Capturing the Local Adsorption Structures of Carbon Dioxide in Polyamine-Impregnated Mesoporous Silica Adsorbents. Journal of Physical Chemistry Letters, 2014, 5, 3183-3187.	4.6	13
203	An Extra‣argeâ€Pore Zeolite with 24×8×8â€Ring Channels Using a Structureâ€Directing Agent Derived fror Traditional Chinese Medicine. Angewandte Chemie, 2018, 130, 6596-6600.	ⁿ 2.0	13
204	A Molecular Ferroelectric Showing Roomâ€Temperature Recordâ€Fast Switching of Spontaneous Polarization. Angewandte Chemie, 2018, 130, 9981-9985.	2.0	13
205	The influence of acid strength and pore size effect on propene elimination reaction over zeolites: A theoretical study. Microporous and Mesoporous Materials, 2019, 278, 121-129.	4.4	13
206	Selective oxidation of methanol over supported vanadium oxide catalysts as studied by solid-state NMR spectroscopy. Journal of Molecular Catalysis A, 2007, 270, 257-263.	4.8	12
207	Origin of Zeolite Confinement Revisited by Energy Decomposition Analysis. Journal of Physical Chemistry C, 2016, 120, 27349-27363.	3.1	12
208	To Be or Not To Be Protonated: <i>cyclo</i> -N ₅ [–] in Crystal and Solvent. Journal of Physical Chemistry Letters, 2018, 9, 7137-7145.	4.6	12
209	Design of Cobalt–Amine Complex as an Efficient Structure-Directing Agent for One-Pot Synthesis of Co-SSZ-13 Zeolite. Journal of Physical Chemistry C, 2021, 125, 16343-16349.	3.1	12
210	Frustrated Lewis Pair in Zeolite Cages for Alkane Activations. Angewandte Chemie - International Edition, 2022, 61, e202116269.	13.8	12
211	A highly selective fluorescent probe for BO ₃ ^{â^`} based on acetate derivatives of coumarin in aqueous solution and thimerosal. Analyst, The, 2013, 138, 813-818.	3.5	11
212	Can Hammett indicators accurately measure the acidity of zeolite catalysts with confined space? Insights into the mechanism of coloration. Catalysis Science and Technology, 2019, 9, 5045-5057.	4.1	11
213	Atom-planting synthesis of MCM-36 catalyst to investigate the influence of pore structure and titanium coordination state on epoxidation activity. Microporous and Mesoporous Materials, 2021, 310, 110645.	4.4	11
214	Electronic‣tate Manipulation of Surface Titanium Activates Dephosphorylation Over TiO ₂ Near Room Temperature. Angewandte Chemie, 2021, 133, 16285-16291.	2.0	11
215	Highly mobile segments in crystalline poly(ethylene oxide)8:NaPF6 electrolytes studied by solid-state NMR spectroscopy. Journal of Chemical Physics, 2014, 140, 074901.	3.0	10
216	New non-metallic mesoporous SBA-15 catalyst with high selectivity for the gas-phase oxidation of cyclohexylamine to cyclohexanone oxime. Catalysis Communications, 2014, 56, 148-152.	3.3	10

#	Article	IF	CITATIONS
217	Recent advances in solid state NMR characterization of zeolites. Chinese Journal of Catalysis, 2015, 36, 789-796.	14.0	10
218	An experimental and quantum mechanical study on luminescence properties of SM(β-Nbm)3·(Pd). Journal of Luminescence, 2012, 132, 1663-1667.	3.1	9
219	Insights into the reaction mechanism of propene H/D exchange over acidic zeolite catalysts from theoretical calculations. Catalysis Science and Technology, 2016, 6, 6328-6338.	4.1	9
220	Design Synthesis of ITE Zeolite Using Nickel–Amine Complex as an Efficient Structure-Directing Agent. ACS Applied Materials & Interfaces, 2018, 10, 33214-33220.	8.0	9
221	Modulation of Selfâ€5eparating Molecular Catalysts for Highly Efficient Biomass Transformations. Chemistry - A European Journal, 2020, 26, 11900-11908.	3.3	9
222	Rational Design of Synergistic Active Sites for Catalytic Ethene/2-Butene Cross-Metathesis in a Rhenium-Doped Y Zeolite Catalyst. ACS Catalysis, 2021, 11, 3530-3540.	11.2	9
223	Electronic‣tate Manipulation of Surface Titanium Activates Dephosphorylation Over TiO ₂ Near Room Temperature. Angewandte Chemie - International Edition, 2021, 60, 16149-16155.	13.8	9
224	Acidic metal–organic framework empowered precise hydrodeoxygenation of bio-based furan compounds and cyclic ethers for sustainable fuels. Green Chemistry, 2021, 23, 9974-9981.	9.0	9
225	Insight into the activation of light alkanes over surface-modified carbon nanotubes from theoretical calculations. Carbon, 2014, 77, 122-129.	10.3	8
226	Mechanistic Pathways for Methylcyclohexane Hydrogenolysis over Supported Ir Catalysts. Journal of Physical Chemistry C, 2014, 118, 20948-20958.	3.1	8
227	Solvent Effect Inside the Nanocage of Zeolite Catalysts: A Combined Solid-State NMR Approach and Multiscale Simulation. Journal of Physical Chemistry C, 2017, 121, 16921-16931.	3.1	8
228	Inspecting the Structure and Formation of Molecular Sieve SAPO-34 via ¹⁷ O Solid-State NMR Spectroscopy. Journal of Physical Chemistry C, 2018, 122, 7260-7277.	3.1	8
229	A nonpolar solvent effect by CH/i€ interaction inside zeolites: characterization, mechanism and concept. Chemical Communications, 2018, 54, 13435-13438.	4.1	8
230	Covalent organic framework shows high isobutene adsorption selectivity from C4 hydrocarbons: Mechanism of interpenetration isomerism and pedal motion. Green Energy and Environment, 2020, 7, 296-296.	8.7	8
231	Confinement-Driven "Flexible―Acidity Properties of Porous Zeolite Catalysts with Varied Probe-Assisted Solid-State NMR Spectroscopy. Journal of Physical Chemistry C, 2021, 125, 11580-11590.	3.1	8
232	Ultra-high concentrations of amino group functionalized nanoporous polymeric solid bases: Preparation, characterization and catalytic applications. Catalysis Communications, 2015, 68, 25-30.	3.3	7
233	Conjugated polymers with defined chemical structure as model carbon catalysts for nitro reduction. RSC Advances, 2016, 6, 99570-99576.	3.6	7
234	Pore-Confined and Diffusion-Dependent Olefin Catalytic Cracking for the Production of Propylene over SAPO Zeolites. Industrial & Engineering Chemistry Research, 2022, 61, 7760-7776.	3.7	7

#	Article	IF	CITATIONS
235	A Heterogeneous Metalâ€Free Catalyst for Hydrogenation: Lewis Acid–Base Pairs Integrated into a Carbon Lattice. Angewandte Chemie, 2018, 130, 13996-14000.	2.0	6
236	¹³ C chemical shift tensors in MOF <i>α</i> â€Mg ₃ (HCOO) ₆ : Which component is more sensitive to hostâ€guest interaction?. Magnetic Resonance in Chemistry, 2020, 58, 1082-1090.	1.9	6
237	Mechanistic insights of selective syngas conversion over Zn grafted on ZSM-5 zeolite. Catalysis Science and Technology, 2020, 10, 8173-8181.	4.1	6
238	Stepwise or Concerted Mechanisms of Benzene Ethylation Catalyzed by Zeolites? Theoretical Analysis of Reaction Pathways. Catalysis Letters, 2021, 151, 3048-3056.	2.6	6
239	Anion-promoted increase of the SiO2/Al2O3 ratio of zeolites. Inorganic Chemistry Frontiers, 0, , .	6.0	6
240	Diffusive Skin Effect in Zeolites. Journal of Physical Chemistry Letters, 2022, 13, 2808-2813.	4.6	6
241	Isomeric Effect on H/D Exchange of Resveratrol Studied by NMR Spectroscopy. Chinese Journal of Chemistry, 2010, 28, 2281-2286.	4.9	5
242	Intactness and spatial proximity of acid–base groups in bifunctional SBA-15 as revealed by solid-state NMR. Chemical Physics Letters, 2010, 491, 72-74.	2.6	5
243	Nano- and Biomaterials for Sustainable Development. Journal of Nanomaterials, 2015, 2015, 1-2.	2.7	5
244	Room temperature stable zinc carbonyl complex formed in zeolite ZSM-5 and its hydrogenation reactivity: a solid-state NMR study. Chemical Communications, 2015, 51, 9177-9180.	4.1	5
245	Direct probing of heterogeneity for adsorption and diffusion within a SAPO-34 crystal. Chemical Communications, 2019, 55, 10693-10696.	4.1	5
246	Waterâ€Induced Structural Dynamic Process in Molecular Sieves under Mild Hydrothermal Conditions: Shipâ€inâ€aâ€Bottle Strategy for Acidity Identification and Catalyst Modification. Angewandte Chemie, 2020, 132, 20853-20862.	2.0	5
247	Correlating the Adsorption Preference and Mass Transfer of Xenon in RHO-Type Molecular Sieves. Journal of Physical Chemistry C, 2021, 125, 6832-6838.	3.1	5
248	Acidity of Solid and Liquid Acids Probed by P-31 NMR Chemical Shifts of Phosphine Oxides. Journal of Analytical Science and Technology, 2011, 2, A155-A158.	2.1	5
249	Single atomic Cu-Anchored 2D covalent organic framework as a nanoreactor for CO2 capture and in-situ conversion: A computational study. Chemical Engineering Science, 2022, 253, 117536.	3.8	5
250	Rational Design of Zirconiumâ€doped Titania Photocatalysts with Synergistic BrÃ,nsted Acidity and Photoactivity. ChemSusChem, 2016, 9, 2759-2764.	6.8	4
251	Solid-State NMR Characterization of the Structure and Catalytic Reaction Mechanism of Solid Acid Catalysts. Wuli Huaxue Xuebao/ Acta Physico - Chimica Sinica, 2017, 33, 270-282.	4.9	4
252	Mapping the dynamics of methanol and xenon co-adsorption in SWNTs by <i>in situ</i> continuous-flow hyperpolarized ¹²⁹ Xe NMR. Physical Chemistry Chemical Physics, 2019, 21, 3287-3293.	2.8	4

#	Article	IF	CITATIONS
253	Thermal Alteration in Adsorption Sites over SAPOâ€34 Zeolite. Angewandte Chemie - International Edition, 2022, 61, .	13.8	4
254	Adsorption Structure and Energy of Pyridine Confined inside Zeolite Pores. Wuli Huaxue Xuebao/ Acta Physico - Chimica Sinica, 2012, 28, 315-323.	4.9	3
255	Frontispiece: New Insight into the Hydrocarbon-Pool Chemistry of the Methanol-to-Olefins Conversion over Zeolite H-ZSM-5 from GC-MS, Solid-State NMR Spectroscopy, and DFT Calculations. Chemistry - A European Journal, 2014, 20, n/a-n/a.	3.3	2
256	Acidity characterization of solid acid catalysts by solid-state 31P NMR of adsorbed phosphorus-containing probe molecules: An update. Annual Reports on NMR Spectroscopy, 2020, , 65-149.	1.5	2
257	Theoretical Prediction from Classical Equations and Rational Synthesis of Ultrafine LTL Zeolite Nanocrystals. Journal of Physical Chemistry C, 2020, 124, 13819-13824.	3.1	2
258	In Situ Observation of Nonâ€Classical 2â€Norbornyl Cation in Confined Zeolites at Ambient Temperature. Angewandte Chemie, 2021, 133, 4631-4637.	2.0	2
259	Gating control effect facilitates excellent gas selectivity in a novel Na-SSZ-27 zeolite. Chemical Communications, 2021, 57, 4170-4173.	4.1	2
260	Frustrated Lewis Pair in Zeolite Cages for Alkane Activations. Angewandte Chemie, 0, , .	2.0	2
261	Towards the Efficient Catalytic Valorization of Chitin to N-Acylethanolamine over Ni/CeO2 Catalyst: Exploring the Shape-Selective Reactivity. Catalysts, 2022, 12, 460.	3.5	2
262	The excited state dynamics study of diâ€2â€pyridylketone in the Aâ€band and Bâ€band absorptions by using resonance Raman spectroscopy, IR and UV–visible spectroscopy. Journal of Raman Spectroscopy, 2012, 43, 1465-1471.	2.5	1
263	Solid-State NMR Characterization of Acidity of Solid Catalysts. , 2018, , 1049-1071.		1
264	A Cationic Oligomer as an Organic Template for Direct Synthesis of Aluminosilicate ITH Zeolite. Angewandte Chemie, 2020, 132, 15779-15785.	2.0	1
265	Precisely regulating the BrÃ,nsted acidity and catalytic reactivity of novel allylic C–H acidic catalysts. Fuel, 2021, 289, 119845.	6.4	1
266	Thermal Alteration in Adsorption Sites over SAPOâ ${\in}34$ Zeolite. Angewandte Chemie, 0, , .	2.0	1
267	Framework aluminum distribution in ZSM-5 zeolite directed by organic structure-directing agents: a theoretical investigation. Catalysis Today, 2022, 405-406, 101-110.	4.4	1
268	Experimental and theoretical study of 13C shielding tensors in new-style molybdenum complex. Science in China Series B: Chemistry, 2004, 47, 214.	0.8	0
269	The Effect of Zirconium Incorporation on the BrÃ,nsted Acidity of Zeolite: A DFT Study. Applied Mechanics and Materials, 0, 44-47, 3616-3619.	0.2	0
270	Innenrücktitelbild: A Heterogeneous Metalâ€Free Catalyst for Hydrogenation: Lewis Acid–Base Pairs Integrated into a Carbon Lattice (Angew. Chem. 42/2018). Angewandte Chemie, 2018, 130, 14131-14131.	2.0	0

#	Article	IF	CITATIONS
271	Rücktitelbild: In Situ Observation of Nonâ€Classical 2â€Norbornyl Cation in Confined Zeolites at Ambient Temperature (Angew. Chem. 9/2021). Angewandte Chemie, 2021, 133, 5004-5004.	2.0	0

272 Solid-State NMR Characterization of Acidity of Solid Catalysts. , 2016, , 1-23.

0